

Electron Spin Resonance on Interacting Donors in Silicon

D. JÉROME AND J. M. WINTER

Centre d'Etudes Nucléaires de Saclay, Service de Physique du Solide et de Résonance Magnétique, Gif-sur-Yvette, Seine-et-Oise, France

(Received 14 November 1963)

The value of the exchange integral J between pairs of donor centers in silicon has been investigated by looking at the ENDOR spectrum of phosphorus-doped silicon in a range of concentration of the order of 8×10^{16} per cc. The microwave field is saturating the cluster electronic line. The line shape of these ENDOR lines gives an unambiguous determination of the sign of this exchange integral which turns out to be anti-ferromagnetic. It is also possible to determine an order of magnitude of J and to have an idea about its distribution for two samples. We are able to understand all the features of the ENDOR spectrum at least in a qualitative way by calculating all the energy levels using a second-order perturbation calculation. A line coming from an ionized phosphorus center, weakly coupled to a pair of neutral phosphorus is also identified.

I. INTRODUCTION

THE substitutional donors like phosphorus or arsenic at low concentration in silicon give rise to a paramagnetic resonance spectrum^{1,2} of $2I+1$ lines,

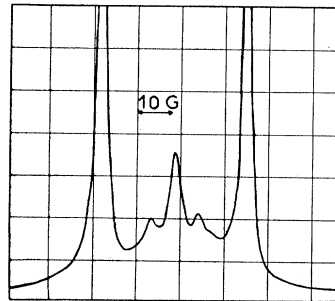


FIG. 1. Electron-resonance spectrum of phosphorus-doped silicon; 8×10^{16} P/cm³ at 1.3°K.

where I is the nuclear spin of the donor ($I = \frac{1}{2}$ for phosphorus). When the concentration of centers is above 6×10^{16} per cc, new lines appear between the $(2I+1)$ lines of the low-concentration spectrum (Fig. 1). Slichter³ gave an explanation for the occurrence of these satellite lines. When two centers are close, there is an overlap between the wave functions of the two electrons, giving rise to an exchange integral, which may be written as $hJ\mathbf{s}_1 \cdot \mathbf{s}_2$, where \mathbf{s}_1 and \mathbf{s}_2 are the electronic spins of the two electrons. We limit ourselves to phosphorus donors from now on. The spectrum is analyzed by diagonalizing the Hamiltonian for a system of four spins $\frac{1}{2}$, two electronic spins \mathbf{s}_1 , \mathbf{s}_2 and two nuclear spins \mathbf{I}_1 and \mathbf{I}_2 . If the value of J is larger than the hyperfine interaction A ,⁴ the total electronic spin defined by $|\mathbf{S}|^2 = |\mathbf{s}_1 + \mathbf{s}_2|^2$ is nearly a good quantum number. We have two electronic states; a triplet $S=1$ and a singlet $S=0$.

The degeneracy of the triplet state is lifted by an

¹ R. C. Fletcher, W. A. Yager, G. L. Pearson, A. N. Holden, W. T. Read, and F. R. Merritt, *Phys. Rev.* **94**, 1392 (1954); R. C. Fletcher, W. A. Yager, G. L. Pearson, and F. R. Merritt, *Phys. Rev.* **95**, 844 (1954).

² G. Feher, R. C. Fletcher, and E. A. Gere, *Phys. Rev.* **100**, 1784 (1955).

³ C. P. Slichter, *Phys. Rev.* **99**, 479 (1955).

⁴ A. Abragam (unpublished lectures).

external magnetic field; we have three electronic sublevels $M_s = +1, 0, \text{ and } -1$. Each of these sublevels has a fourfold nuclear degeneracy, partially lifted by the hyperfine coupling and the nuclear Zeeman energy. The energy level of the singlet state crosses one of the triplet sublevels for a certain value of the external field (Fig. 2). As the hyperfine coupling has matrix elements between singlet and triplet states, in the vicinity of the crossing, there will be large change of energy levels and wave functions. By studying with the ENDOR technique, the structure of the nuclear sublevels, and the magnitude and the sign of J will be determined. The microwave field at 9206 Mc/sec is saturating the cluster electronic line, therefore we select nuclear spins of pairs of exchange-coupled phosphorus nuclei (Fig. 1). In a given sample, there is a distribution of values of J due to the random distribution of phosphorus centers. We have been able to determine the value of J which has the largest probability for two samples with different phosphorus concentrations.

II. THEORY

1. First-Order Perturbation Theory of Energy Levels

We assume that the overlap of the wave functions belonging to two neighboring phosphorus atoms, leads

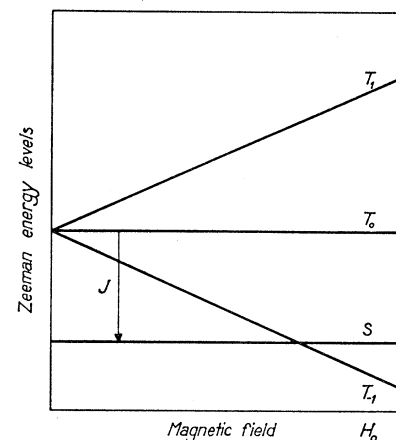


FIG. 2. Energy levels of the system of two electronic spins in the static magnetic field coupled by the exchange interaction.

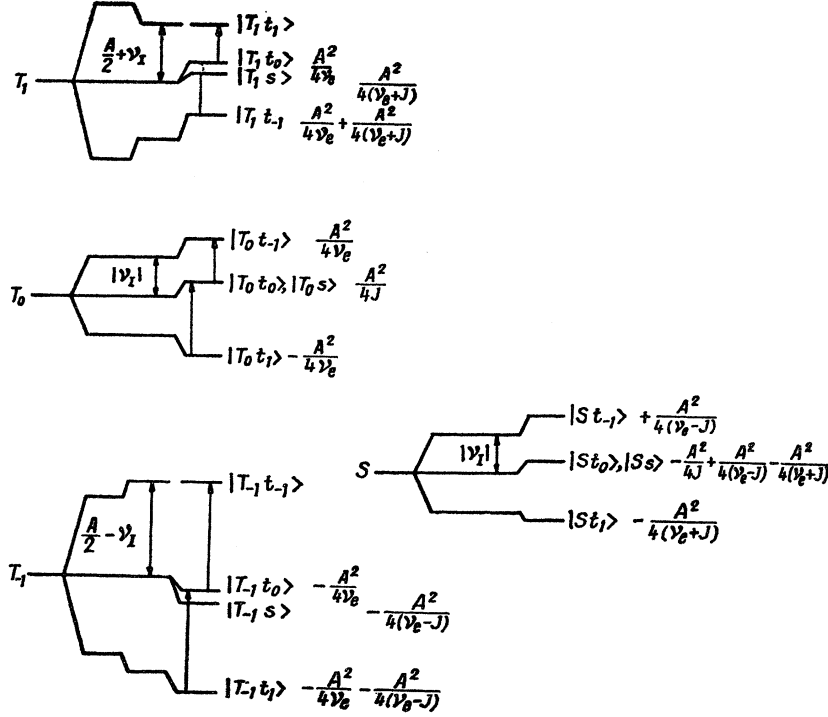


FIG. 3. Second-order shift of energy nuclear sublevels in the different triplet and singlet electronic states (not to scale). The good wave functions in zero-order approximation are noted beside each level. We assume an antiferromagnetic coupling lower than ν_e .

to a coupling between their spins $hJ\mathbf{s}_1 \cdot \mathbf{s}_2$. The total Hamiltonian will be written in frequency units.⁴

$$\mathcal{H}C = \nu_e(s_{1z} + s_{2z}) + J\mathbf{s}_1 \cdot \mathbf{s}_2 + A(\mathbf{s}_1 \cdot \mathbf{I}_1 + \mathbf{s}_2 \cdot \mathbf{I}_2) + \nu_I(I_{1z} + I_{2z}), \quad (1)$$

where ν_e and ν_I are the electronic and nuclear Larmor frequencies, respectively. J is the exchange coupling value which has been measured in cycles per second.⁵

To a first approximation, taking into consideration only the first two terms of the Hamiltonian (1), the total electronic spin is a good quantum number:

$$|S|^2 = |\mathbf{s}_1 + \mathbf{s}_2|^2 \quad \text{and} \quad S_z = s_{1z} + s_{2z}$$

define good quantum numbers.

The Zeeman electronic Hamiltonian removes the degeneracy of the triplet state $S=1$ and gives the three following electronic states:

$$|T_1\rangle, \quad M_s = +1; \quad |T_0\rangle, \quad M_s = 0; \quad |T_{-1}\rangle, \quad M_s = -1.$$

The singlet state $|S\rangle$, $S=0$ is diamagnetic. In the spin multiplicity $S=1$, \mathbf{s}_1 and \mathbf{s}_2 may be replaced by $\mathbf{S}/2$. This gives for the Hamiltonian of the whole system:

$$\mathcal{H}C = \nu_e S_z + \frac{1}{4}J + \frac{1}{2}A\mathbf{S} \cdot (\mathbf{I}_1 + \mathbf{I}_2) + \nu_I(I_{1z} + I_{2z}). \quad (2)$$

In lowest order, the energy of (2) will be given by

$$E_{M_s m_1 m_2} = \frac{1}{4}J + \nu_e M_s + \frac{1}{2}A M_s (m_1 + m_2) + \nu_I (m_1 + m_2).$$

⁵ From now on, we assume a positive value for J . We shall see further that this hypothesis will be verified.

In the Hamiltonian (1), ν_e and A are positive quantities and ν_I is negative for a positive nuclear moment as that of P^{31} . The first-order energy levels are shown in Fig. 3. The electronic transition frequencies $\Delta S=0$, $\Delta M_s = \pm 1$, $\Delta m_1 = \Delta m_2 = 0$ are the following:

$$\nu = \nu_e + \frac{1}{2}A(m_1 + m_2).$$

The electronic resonance spectra exhibit two lines at frequencies $\nu_e \pm \frac{1}{2}A$ which are not observable, due to the lines of the isolated donors and a line at the frequency ν_e twice as intense corresponding to $m_1 + m_2 = 0$.^{2,4}

We use the same considerations for clusters of three phosphorus atoms in the spin multiplicity $S = \frac{3}{2}$ which is completely symmetric with respect to the three spins \mathbf{s}_1 , \mathbf{s}_2 , and \mathbf{s}_3 . We obtain for this case $\mathbf{s}_1 = \mathbf{s}_2 = \mathbf{s}_3 = \frac{1}{3}\mathbf{S}$. The only electronic frequencies are $\nu_e \pm \frac{1}{2}A$ and $\nu_e \pm \frac{1}{6}A$.

The two eigenstates of spin $S = \frac{1}{2}$ give electronic resonance frequencies which vary from one cluster to another giving rise to a continuous background as has been shown by Abragam.⁴

The only discrete lines for four-atom clusters are ν_e , $\nu_e \pm \frac{1}{2}A$, $\nu_e \pm \frac{1}{4}A$. A line at frequency ν_e broadened by hyperfine interaction with Si^{29} spins appears only for clusters of an even number of phosphorus atoms.

At a temperature of 1.3°K the electronic resonance spectrum shows lines at frequencies $\nu_e \pm \frac{1}{2}A$ which merge almost completely in the background line. We conclude that the number of four-atom clusters is negligible in the samples (Fig. 1).

TABLE I. Allowed nuclear transitions and ENDOR frequencies.

$ T_{-1,t_0}\rangle \rightarrow T_{-1,t_{-1}}\rangle$	$\frac{A}{2} - \nu_I + \frac{A^2}{4\nu_e}$	$ T_{1,t_0}\rangle \rightarrow T_{1,t_1}\rangle$	$\frac{A}{2} + \nu_I - \frac{A^2}{4\nu_e}$	$ T_{0,t_1}\rangle \rightarrow T_{0,t_0}\rangle$	$ \nu_I + \frac{A^2}{4\nu_e} + \frac{A^2}{4J}$
$ T_{-1,t_1}\rangle \rightarrow T_{-1,t_0}\rangle$	$\frac{A}{2} - \nu_I + \frac{A^2}{4(\nu_e - J)}$	$ T_{1,t_{-1}}\rangle \rightarrow T_{1,t_0}\rangle$	$\frac{A}{2} + \nu_I - \frac{A^2}{4(\nu_e + J)}$	$ T_{0,t_0}\rangle \rightarrow T_{0,t_{-1}}\rangle$	$ \nu_I + \frac{A^2}{4\nu_e} - \frac{A^2}{4J}$

2. Second-Order Perturbation Theory of Energy Levels

There are nondiagonal matrix elements of the hyperfine structure Hamiltonian $\mathcal{H}_P = A(\mathbf{I}_1 \cdot \mathbf{s}_1 + \mathbf{I}_2 \cdot \mathbf{s}_2)$ between different triplet states and between singlet and triplet states. The O_z component of the total spin $F_z = S_z + I_{1z} + I_{2z}$ and the total symmetry of wave functions with respect to interchange of two atoms are good quantum numbers. We defined a total parity number P as negative when the sign of the wave function changes by simultaneous permutation of the two electronic spins and the two nuclear spins. The perturbed states will be classified according to the two good quantum numbers as indicated in Fig. 3.

The coupling of nuclear spins in every electronic level gives three symmetric triplet states $|t_1\rangle$, $|t_0\rangle$, and $|t_{-1}\rangle$, and an antisymmetric singlet state $|s\rangle$. The even-interaction \mathcal{H}_P couples states which have same quantum numbers F_z and the same total parity. This is true for any order perturbation calculation.

Starting with the eigenfunctions of zero order (Fig. 3), we obtain immediately the nondiagonal matrix elements from which one can obtain the shift of energy levels.

We present the calculation of the shift for triplet states $|T_1\rangle$ and $|T_0\rangle$. We deduce shifts of $|T_{-1}\rangle$ levels by exchanging ν_e in $-\nu_e$ in the formula.

(a) $|T_{1,t_1}\rangle$. This state is not coupled with any other state triplet or singlet because $|T_{1,t_1}\rangle$ is the only state with $F_z = 2$ and there is no change in its energy beyond the first-order value.

(b) $|T_{1,t_0}\rangle$ and $|T_{1,s}\rangle$. $|T_{1,t_0}\rangle$ is coupled to $|T_{0,t_0}\rangle$ and $|T_{1,s}\rangle$ to $|S,t_1\rangle$ by the nondiagonal matrix elements. There are no diagonal matrix elements for any of these states,

$$\begin{aligned} \langle T_{1,t_0} | \mathcal{H}_P | T_{0,t_1} \rangle &= A/2, \\ \langle T_{1,s} | \mathcal{H}_P | S,t_1 \rangle &= -A/2. \end{aligned}$$

The second-order shift of the state $|T_{1,s}\rangle$ is

$$E = A^2/4(\nu_e + J),$$

and that of state $|T_{1,t_0}\rangle$ is

$$E = A^2/4\nu_e.$$

(c) $|T_{1,t_{-1}}\rangle$. This state is coupled to $|T_{0,t_0}\rangle$ and $|S,s\rangle$. Its shift is

$$A^2/4\nu_e + A^2/4(\nu_e + J).$$

(d) $|T_{0,t_0}\rangle$ and $|T_{0,s}\rangle$. The same method as that of Sec. 2(b) does not remove the degeneracy between the two states in second order. To that order both states are shifted by the same amount,

$$E = A^2/4J.$$

(e) $|T_{0,t_1}\rangle$ and $|T_{0,t_{-1}}\rangle$. The shifts are respectively $A^2/4\nu_e$ and $-A^2/4\nu_e$. This computation is only valid under conditions: $A \ll \nu_e, J, \nu_e - J, \nu_e + J$. It is not valid at the crossing of energy levels. This restriction is important as we shall see further.

3. Line Shapes and Frequencies of Nuclear Transitions

(a) The coupling with the rf field inducing an electronic or nuclear transition is an operator proportional to

$$\alpha(s_{1x} + s_{2x}) + \beta(I_{1x} + I_{2x}).$$

The selection rules for electronic or nuclear transitions are thus $\Delta F_z = \pm 1, \Delta P = 0$. With a perturbation like $s_{1x} + s_{2x}$ or $I_{1x} + I_{2x}$ the total parity is preserved. The allowed transitions are shown in Table I and Fig. 3.

(b) From Table I, it appears that nuclear lines are

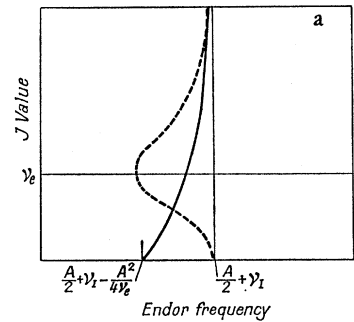
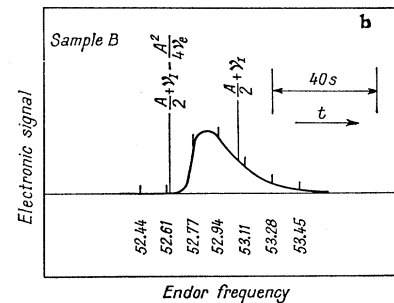


FIG. 4. (a)—Theoretical dependence on J of the ENDOR frequency in the group $\frac{1}{2}A + \nu_I$ and estimate of J distribution in dashed line. (b)—Experimental line shape for sample B.



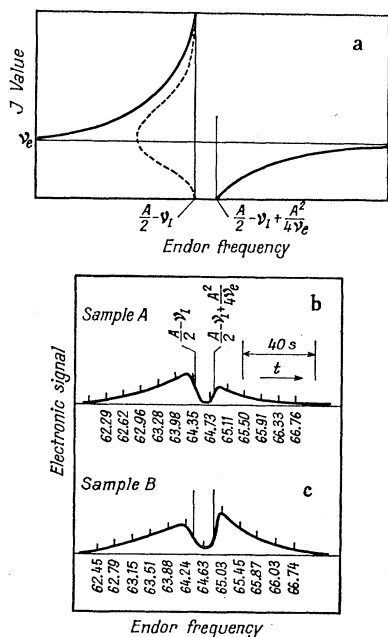


FIG. 5. (a)—Theoretical dependence on J of the ENDOR frequency in the group $\frac{1}{2}A - \nu_I$ and estimate of J distribution in dashed line. (b)—Experimental line shape for samples A and B, respectively, showing the frequency gap.

split into three groups, two whose frequencies in first order are $\frac{1}{2}A - \nu_I$ and $\frac{1}{2}A + \nu_I$, and one whose mean frequency is near the Larmor frequency of a bare phosphorus atom. We assume now $J > 0$. The values of the coupling constant are distributed in the clusters with a distribution function $P(J)$ normalized to unity when J is varied from zero to infinity. It is assumed to have a maximum for a value $J = J_P$.

The $\frac{1}{2}A + \nu_I$ group includes two frequencies. One is J -independent $\frac{1}{2}A + \nu_I - (A^2/4\nu_e)$, the other is J -dependent $\frac{1}{2}A + \nu_I - [A^2/4(\nu_e + J)]$. The distribution of J produces a distribution of the latter frequencies (Fig. 4). The $\frac{1}{2}A - \nu_I$ group always includes one J -independent frequency line. The others show a singular energy denominator for $J = \nu_e$. Thus, a second-order perturbation-frequency treatment is no longer valid for such clusters ($J \approx \nu_e$) far from $\frac{1}{2}A - \nu_I$, are not observed. It is important to notice that there is a forbidden frequency band of width $A^2/4\nu_e$ in the $\frac{1}{2}A - \nu_I$ group. Such a phenomenon does not occur in the $\frac{1}{2}A + \nu_I$ group assuming an antiferromagnetic coupling (Figs. 4 and 5). The $|\nu_I|$ group includes two lines whose frequencies are J -dependent (Fig. 6).

III. EXPERIMENTAL

1. Principles of the Experiment

A microwave field at the frequency $\nu_e = 9206$ Mc/sec is applied. The populations of the electronic levels corresponding to the nuclear sublevels $m_1 + m_2 = 0$ are therefore equalized. Then a rf field of frequency ν in the vicinity of one of the nuclear-transition frequencies is also applied. This field produces a change in the

population of one of the states with $m_1 + m_2 = 0$ and the electronic signal varies. By sweeping the radio-frequency ν we reach all the nuclear frequencies possible.⁶ For a given ν the change of the electronic signal is very likely proportional to the number of clusters having the nuclear frequency transition ν . For instance, if we look at the ENDOR frequencies $\nu_I + (A^2/4\nu_e) \pm (A^2/4J)$, the spectrum reproduces the distribution of the values of $A^2/4J$ in our sample.

2. Experimental Technique

The frequency of the electronic spectrometer is stabilized by a Pound discriminator on an external cavity. We use a constant-level symmetric detection.⁷ All these experiments have been done at 1.3°K and because of the length of the electronic relaxation time, the dispersion mode is observed.⁶ The signal-to-noise ratio for the ENDOR signal on clusters varies between 3 and 5. We use two samples of phosphorus-doped silicon from Merck;

Sample A: $N = 8 \times 10^{16}$ P/cc $\rho = 0.11 \Omega\text{-cm}$,

Sample B: $N = 6 \times 10^{16}$ P/cc $\rho = 0.13 \Omega\text{-cm}$.

3. Experimental Results

Taking for the phosphorus nuclear Larmor frequency the value $|\nu_I| = 5.67$ Mc/sec and for the hyperfine constant the value⁶ $A = 117.53$ Mc/sec, the nuclear-frequency transition calculated in a first-order approximation is given by $\frac{1}{2}A - \nu_I = 64.11$ Mc/sec, $\frac{1}{2}A + \nu_I = 53.09$ Mc/sec, and $|\nu_I|$. A typical second-order correction is given by $A^2/4\nu_e = 0.375$ Mc/sec.

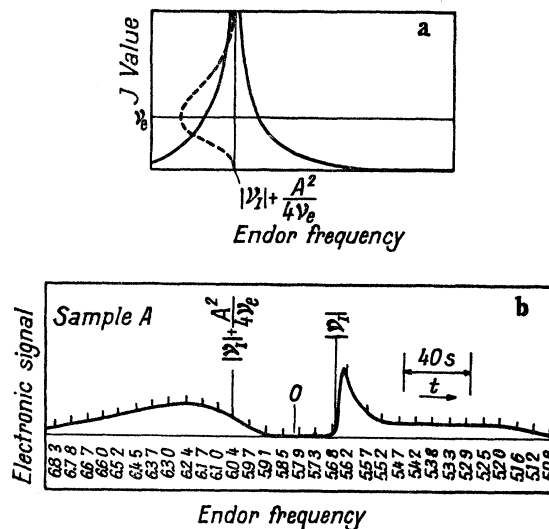


FIG. 6. (a)—Theoretical dependence on J of the ENDOR frequency in the group $|\nu_I|$. (b)—Experimental line shape for sample A.

⁶ G. Feher, Phys. Rev. **114**, 1219 (1959).

⁷ G. Feher, Bell System Tech. J. **26**, 449 (1957).

The ENDOR line in the vicinity of $\nu = \frac{1}{2}A - \nu_I$ shows two peaks separated by a frequency gap of the order of $A^2/4\nu_e$. This fact shows without any ambiguity that the singlet level crosses the group of $M_s = -1$ sublevels and the coupling is antiferromagnetic (Fig. 5).

The line for $M_s = 1$ sublevels shows only a broadening (Fig. 4) coming from the different possible value of the second-order shift $A^2/4(\nu_e + J)$.

The ENDOR line for the $M_s = 0$ group of levels (Fig. 6) occurs at the frequencies ν given by $\nu = |\nu_I| + (A^2/4\nu_e) \pm (A^2/4J)$.

As stated above, the shape of the line reproduces the distribution of $A^2/4J$. If we call J_P the value of J which gives the maximum probability for $A^2/4J$, we deduce $A^2/2J_P$ by measuring the distance between the maximum of the two peaks. For the sample A we find

$$A^2/2J_P = 0.94 \text{ Mc/sec.}$$

Knowing the distribution for $A^2/4J$, it is possible to deduce the function $P(J)$, giving the probability of finding a given J and in particular, the value J_P giving the maximum value for $P(J)$. The results are

$$\text{Sample A: } J_P = 15\,000 \pm 3\,000 \text{ Mc/sec,}$$

$$\text{Sample B: } J_P = 13\,500 \pm 3\,000 \text{ Mc/sec.}$$

The shape of the two other lines can be discussed in a qualitative way. Figure 5 shows the lines $\frac{1}{2}A - \nu_I$ for the two samples; for the sample A the low-frequency peak is more intense than the high-frequency peak. The result is opposite for sample B.

Since the low-frequency peak corresponds to values of J larger than ν_e and the other peak to values of J smaller than ν_e , this result is consistent with the fact that J_P is smaller in sample B than in sample A (Fig. 5).

The width of the experimental frequency gap is smaller than $A^2/4\nu_e$; the time constant due to electronic saturation is probably reducing the experimental gap.

Coming back to the line at ν_I we notice (Fig. 6) the two broad lines. The intensity of these lines is very small in sample B. The width of the line, being of the order of $A^2/4J_P$, is larger for sample B and is responsible for the small signal.

IV. INFLUENCE OF IONIZED CENTERS

A very narrow line (10 kc/sec) occurring exactly at the frequency $|\nu_I|$ is observed in the ENDOR spectrum of both samples (Fig. 6). Feher⁶ already noticed the occurrence of this line in the ordinary ENDOR spectrum of a compensated sample and attributed it to an ionized phosphorus center.

Assuming that there is an ionized phosphorus in the vicinity of a cluster of two neutral phosphorus, there always will be a small scalar coupling between the two electronic spins and the ionized phosphorus nuclear spin I' . We therefore add, to our Hamiltonian (1), the term

$$a_1 I' \cdot \mathbf{s}_1 + a_2 I' \cdot \mathbf{s}_2 + \nu_I I'_z'$$

This coupling comes because the wave function for the two electrons localized around phosphorus 1 and 2, has a small admixture of a wave function for an electron bound to the phosphorus I' . This is an extension to a system of three phosphorus and two electrons of the calculation performed by Miller and Abrahams⁸ for explaining the conduction of compensated sample. Because the admixture is very small a_1 and a_2 are much smaller than A . This new term gives a contribution to the energy spectrum, which is for a state M_s (of the triplet):

$$\nu_I m' + \frac{1}{2}(a_1 + a_2) m' M_s,$$

m' being the value of I'_z' .

As a_1 and a_2 are small this term does not influence the electronic spectrum. But there are now ENDOR lines corresponding to the selection rule $\Delta m' = \pm 1$, and occurring at frequencies given by

$$\nu = |\nu_I| + \frac{1}{2}(a_1 + a_2) M_s$$

(we neglect second-order corrections). For $M_s = 0$ a line appears exactly at $\nu = |\nu_I|$.

There are also ENDOR lines corresponding to value of $M_s = \pm 1$, but they are not observed because there is a distribution of a_1 and a_2 values.

The important point is to notice that only lines corresponding to the $M_s = 0$ level of clusters are observed. There is undoubtedly phosphorus ionized near isolated neutral phosphorus, but their ENDOR frequencies are given by $\nu = |\nu_I| + \frac{1}{2}aM_s$, $M_s = \pm \frac{1}{2}$ and are not observed. We observe only ionized phosphorus coupled to clusters of two neutral phosphorus, this point is also proved by the following experimental fact.

Now we saturate the electronic line $\nu = \nu_e \pm \frac{1}{2}A$ (Fig. 1) and look at the ENDOR spectrum. The narrow line at $|\nu_I|$ appears but its intensity is half the intensity of the $|\nu_I|$ line observed when we saturate the $\nu = \nu_e$ line. It is known that a cluster of two has an electron spectrum with lines at $\nu = \nu_e \pm \frac{1}{2}A$ which are not observed because they are masked by the large signal coming from isolated phosphorus, the intensity of these lines is one-half the intensity of the $\nu = \nu_e$ central line. So the narrow $\nu = |\nu_I|$ line observed when we saturate the electronic lines at $\nu = \nu_e \pm \frac{1}{2}A$ is not due to the ENDOR spectrum of isolated phosphorus but to the ENDOR spectrum of clusters of phosphorus.

By comparing the intensity of the narrow $\nu = |\nu_I|$ line and the intensity of the broad line near $|\nu_I|$ (coming from neutral phosphorus) it should be possible to get quantitative informations about the degree of compensation of the samples.

V. THEORETICAL ESTIMATE OF THE EXCHANGE ENERGY

The Hamiltonian of the two-electron system is given by

$$\mathcal{H}(1,2) = T(\mathbf{r}_1) + T(\mathbf{r}_2) + V_i(\mathbf{r}_1) + V_j(\mathbf{r}_1) + V_i(\mathbf{r}_2) + V_j(\mathbf{r}_2) + V(\mathbf{r}_1, \mathbf{r}_2),$$

⁸ A. Miller and E. Abrahams, Phys. Rev. **120**, 745 (1960).

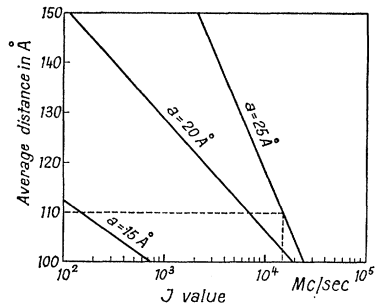


FIG. 7. Results of the computation of J as a function of the average distance between two neighboring donors. The experimental value of J for sample A corresponds to an average distance of 110 Å, assuming $a=25$ Å.

where \mathbf{r}_1 and \mathbf{r}_2 are the coordinates of the two electrons, $T(\mathbf{r})$ is the kinetic-energy operator, $V_i(\mathbf{r})$ and $V_j(\mathbf{r})$ are the attractive potentials due to phosphorus nuclei at sites i and j . In our spin Hamiltonian (1), J is defined as the energy difference between triplet and singlet spin states^{9,10}

$$J = \langle T | \mathcal{H}(1,2) | T \rangle - \langle S | \mathcal{H}(1,2) | S \rangle,$$

where $|T\rangle$ is the total wave function for the system, antisymmetric with respect to the orbital variables, symmetric with respect to the spin variables in the triplet spin state. The opposite is true for $|S\rangle$.

The orbital part of the one-electron wave function, taken from the effective-mass theory¹¹ may be written at a site i :

$$\psi_i(\mathbf{r}) = \sum_{p=1}^6 (6)^{-1/2} F_p(\mathbf{r}) \phi_p(\mathbf{r}),$$

where $\phi_p(\mathbf{r})$ is a Bloch function corresponding to the wave vector of the p valley, and $F_p(\mathbf{r})$ is an envelope function satisfying the wave equation in the effective-mass approximation:

$$F_p(\mathbf{r}) = (\pi a^2 b)^{-1/2} \exp \left[- \left[\frac{x^2 + y^2}{a^2} + \frac{z^2}{b^2} \right]^{1/2} \right],$$

the z axis being parallel to the wave vector corresponding to the value p . In silicon a and b are¹²

$$a = 25 \text{ Å}, \quad b = 14.2 \text{ Å}.$$

According to our definition of the exchange energy, J takes the following form⁹:

$$J = -2 \int \psi_i^*(\mathbf{r}_1) \psi_j(\mathbf{r}_1) \int \psi_j^*(\mathbf{r}_2) V(\mathbf{r}_2) \psi_i(\mathbf{r}_2) d\mathbf{r}_1 d\mathbf{r}_2 \\ - \int \psi_i^*(\mathbf{r}_1) \psi_j(\mathbf{r}_1) \frac{e^2}{\kappa_0} |\mathbf{r}_1 - \mathbf{r}_2|^{-1} \psi_j^*(\mathbf{r}_2) \psi_i(\mathbf{r}_2) d\mathbf{r}_1 d\mathbf{r}_2.$$

⁹ P. W. Anderson, in *Solid State Physics*, edited by F. Seitz and D. Turnbull (Academic Press Inc., New York, 1963), Vol. 14.

¹⁰ W. Heitler and F. London, *Z. Physik* **44**, 455 (1927).

¹¹ J. M. Luttinger and W. Kohn, *Phys. Rev.* **97**, 869 (1955).

¹² W. Kohn, in *Solid State Physics*, edited by F. Seitz and D. Turnbull (Academic Press Inc., New York, 1957), Vol. 5.

Since $V(\mathbf{r}_2)$ is an attractive potential the first term is a positive one, the second is negative. If one neglects the anisotropy of the envelope function within a given valley, the estimate of J is simple. But one should notice that each term of the latter expression is smaller than the one obtained by using a pure hydrogenic wave function because there is destructive interference between parts of the wave functions coming from different valleys.

Utilizing Eq. (II 17), Eq. (II 18), and (paragraph) IV of Ref. 8, we evaluated J (as function of the distance between phosphorus centers) assuming an isotropic envelope function and taking for the radius $a=25$, 20, or 15 Å (Fig. 7). We find that the positive theoretical value of J agrees with the experimental results. The average distance between centers is easily deduced from the concentration of centers, and we find that the experimental value of J is larger than the theoretical prediction, even if we use $a=25$ Å for the radius. If we believe in the impurity concentration measurements by conductivity at room temperature, this fact seems to indicate that the average distance between donors is smaller than the average distance deduced from the concentration, by about 20%. This may be due to a nonuniform concentration of phosphorus donors. It has been suggested that impurities tend to concentrate along dislocation lines.¹³

VI. CONCLUSION

The method we described can only give information if the exchange integral is larger than the hyperfine coupling A , otherwise no electronic line at the frequency ν_e appears in the spectrum. There is also an upper limit because when J becomes larger than kT and $h\nu_e$; there are very few electrons in the triplet states. If we remark that J varies very rapidly with the distance, our method is only valid in a narrow range of concentration. At high concentration, another limit appears. The electronic relaxation time becomes shorter, and the line difficult to saturate.

The possibility of measuring J is directly related to the presence of the hyperfine coupling term; without it, the exchange term and the Zeeman term commute and the frequencies are not affected by the exchange term. It is the small coupling by the hyperfine energy of the triplet and singlet levels which allows measurement of J . The effect of exchange on the energy spectrum is very small except when the crossing occurs. By a second-order perturbation calculation we are able to explain the shape of the experimental ENDOR spectrum and to determine the sign and the magnitude of J .

We have explained the occurrence of an ENDOR line

¹³ D. K. Wilson, Ph.D. dissertation, Rutgers University, New Brunswick, New Jersey, May 1963 (unpublished).

coming from an ionized phosphorus center weakly coupled to a cluster of two neutral phosphorus atoms.

Note added in proof. Dr. J. J. Pearson made a calculation of J without neglecting the anisotropy of the envelope function. The results will be published in a separate article.

ACKNOWLEDGMENTS

The authors are especially indebted to Professor A. Abragam for very helpful suggestions, and to Dr. Ch. Ryter and Dr. C. Robert for their help on the experimental part of this work.

Peierls Stress and Creep of a Linear Chain*

J. H. WEINER AND W. T. SANDERS

Department of Mechanical Engineering, Columbia University, New York, New York

(Received 19 December 1963; revised manuscript received 23 January 1964)

The Frenkel-Kontorova dislocation model is modified by replacing the sinusoidal substrate force by one which is piecewise linear. Exact solutions are found for the static configuration and for the Peierls stress, σ_P . Good agreement is found between these values of σ_P and those obtained previously for a two-dimensional Rosenstock-Newell model. The atoms of the linear chain are then considered in random motion corresponding to thermal equilibrium and under an applied stress $\sigma < \sigma_P$. The time required for motion of the dislocation from one position of stable equilibrium to an adjacent one is computed by means of a rate-theory formulation adapted to the present type of problem in which the positions of all the atoms in the chain are required to vary in passing over the potential barrier. The theoretical transition times for an infinite chain are compared with analog computer results for a six-atom chain and reasonably good agreement is found.

1. INTRODUCTION

THE rate of dislocation creep over the Peierls barrier has been studied in connection both with low-temperature creep¹ and the Bordoni peak.² Because of the complexity of the phenomenon, it is necessary to make various assumptions of a mathematical and physical nature when treating a realistic model of the process.

The purpose of the present work has been to construct a simple dislocation model which is amenable to analysis with few additional assumptions. It is hoped that the results of this idealized analysis may provide insight into the nature of the real process, and that the mathematical techniques employed may be applied to more realistic models.

The dislocation model considered here is a modification of the Frenkel-Kontorova one-dimensional model³ with the sinusoidal substrate force replaced by one which is piecewise linear as in the two-dimensional treatment of Sanders.⁴ For this model it is possible to

obtain exact solutions to the difference equation describing the static configuration under applied stress and to derive an exact expression for the Peierls stress, σ_P (Sec. 2). The values of σ_P computed here agree surprisingly well with the results of the two-dimensional calculations.⁴

In order to study the dislocation creep rate, the atoms of the model are then considered in random motion corresponding to thermal equilibrium and under an applied stress $\sigma < \sigma_P$. The problem of determining the rate at which the dislocation passes from one stable equilibrium position to an adjacent one is in the general class of problems considered in rate theory.⁵ We present here (Sec. 3) a derivation of the pertinent rate formula *ab initio* which is somewhat different from the usual one and is particularly adapted to the present type of problem in which the positions of all the atoms in the chain are required to vary in passing over the potential barrier.

For the infinite chain dislocation model it is possible (Sec. 4) to calculate explicitly all the quantities entering into this rate formula. The theoretically predicted values of the frequency of transition of the dislocation from one equilibrium position to an adjacent one are found to be in order-of-magnitude agreement with analog

* This research was supported jointly by the U. S. Air Force Office of Scientific Research under Grant No. AF-AFOSR-228-63 and by the National Science Foundation under Grant No. NSF-G19010.

¹ J. Lothe and J. P. Hirth, *Phys. Rev.* **115**, 543 (1959).

² A. Seeger, H. Donth, and F. Pfaff, *Discussions Faraday Soc.* **23**, 19 (1957).

³ J. Frenkel and T. Kontorova, *Phys. Z. Sowjetunion* **13**, 1 (1938); *J. Phys. (U.S.S.R.)* **1**, 137 (1939). A paper which appeared after this manuscript was submitted [J. Kratochvil and V. L. Indenbom, *Czech. J. Phys.* **13**, 814 (1963)] treats the same modification of the Frenkel-Kontorova model from the static viewpoint only.

⁴ W. T. Sanders, *Phys. Rev.* **128**, 1540 (1962).

⁵ H. Eyring, *J. Chem. Phys.* **3**, 107 (1935); C. Wert and C. Zener, *Phys. Rev.* **76**, 1169 (1949); C. Wert, *ibid.* **79**, 601 (1950). A paper which came to our attention after this manuscript was submitted is G. H. Vineyard, *Phys. Chem. Solids* **3**, 121 (1957), which also develops the pertinent rate formula from the viewpoint of Sec. 3. We have retained the present discussion, which differs somewhat in emphasis, for the sake of completeness.